Multiple Interactions at HERA

H. Jung[a]*, Ll. Marti*[a]*, T. Namsoo*[a]*, S. Osman*[b]

[a] DESY, Hamburg, Germany
[b] Physics Department, University of Lund, Lund, Sweden

Abstract

The study of Multiple Parton Interactions (MPI) has been an important subject at hadron colliders. In lepton-hadron collisions at HERA, the photon can interact as a point-like particle or as a composite hadron-like system. Event samples with an enriched direct- or resolved-photon component can be selected by choosing events with high or low x_γ or Q^2 values. This was done in the three measurements presented here, which were conducted at HERA by the H1 and ZEUS collaborations. Two measurements in photoproduction are presented. The first looks at three- and four-jet events and the second, at the charged particle multiplicity in dijet events. Also presented is a measurement of the multiplicity of low p_T jets in inclusive one-jet deep inelastic scattering events. In all three analyses possible effects of MPI were found.

1 Introduction

In ep collisions at HERA the mediator boson was a virtual photon[1] which can be characterized by two variables namely, the photon virtuality, Q^2, and the inelasticity, y. The life-time of an $e\gamma$-state is of the order $\sim 1/Q^2$. Within this life-time the photon can develop $q\bar{q}$-fluctuations. The life-time of these fluctuations are constant as a function of the characteristic p_T of the interacting partons and are of the order $\sim 1/p_T^2$. Therefore, these fluctuations are important only if $Q^2 \ll p_T^2$. In this case, the photon can fluctuate into a $q\bar{q}$ pair or even more complicated states and these events have similar characteristics to hadron-hadron collisions.

QCD Monte Carlo programs (MC) simulate ep collisions at leading order in α_s, $\mathcal{O}(\alpha\alpha_s)$, with a 2-to-2 parton scattering. The events are simulated with initial as well as final parton state radiation and the contributions from the break up of the proton. Finally, hadronisation models are applied so that colourless particles are produced. In this picture, the primary two hard partons lead to two jets. The underlying event is defined as everything except the lowest order process. Ideally, the lowest order process is not affected by the underlying event but experimentally contributions from the underlying event are present in these jets and cannot be disentangled. The underlying event is therefore the initial and final state radiation and the remnant-remnant interactions as well as re-scatters off the remnants. These two last contributions are referred to as multiple parton interactions (MPI). In perturvative Quantum Chromodynamics (pQCD), the AGK cutting rules [1–3] can be used to relate the different contributions to ep scattering, diffraction and single or multiple scattering, via multiple exchange of BFKL Pomerons.

[1] For the photon virtuality range considered in these analyses.

Remnant-remnant interactions can only be present if the interacting particles have a composite structure via multi-parton exchange. In lepton-proton collisions this is only possible if the photon is resolved. The fraction of the photon energy entering in the hard scattering x_γ may be used to select enriched samples by resolved or point-like (direct) photons. Thus, at LO parton level, $x_\gamma = 1$ for direct processes whereas in the resolved case, $x_\gamma < 1$. Experimentally, the variable x_γ^{obs} is used. It is defined in terms of the two hardest jets, Jet_1 and Jet_2, and the hadronic final state (HFS) as:

$$x_\gamma^{obs} = \frac{\sum_{h \in Jet_1}(E - P_z) + \sum_{h \in Jet_2}(E - P_z)}{\sum_h (E - P_z)}, \tag{1}$$

where the sums in the nominator run over the hadrons in Jet_1 and Jet_2, while the sum in the denominator runs over all hadrons in the entire HFS.

In the past, the underlying event was studied at HERA in the photoproduction regime [4,5] but not in deep inelastic scattering (DIS). The next sections are organized as follows. Firstly, a three- and four-jet cross section measurement in photoproduction is presented. Then two different analyses with similar strategies are shown, in which four regions in the azimuthal angle ϕ are defined with respect to the leading jet, i.e. that with the highest E_T in the event. The first of these analyses is a charged particle multiplicity measurement in dijet photoproduction. The second is a mini-jet multiplicity measurement in DIS, where a mini-jet refers to a jet with low transverse momentum.

2 Three- and four-jet events in photoproduction

The leading order for an n-jet event, via a single chain exchange, is $\mathcal{O}(\alpha\alpha_s^{n-1})$. However, n-jet events can also be generated via MPI, where several chains are present. Moreover, even soft MPI may affect the distribution of multi-jet events by adding or redistributing the energy flow generated by a primary process.

The ZEUS collaboration studied the multi-jet production in the photoproduction regime [6], where $Q^2 < 1$ GeV^2 and $0.2 < y < 0.85$. Three- and four-jet events, where the jets were defined with the k_T clustering algorithm [7] and require to have transverse energies $E_T^{jets} > 6$ GeV, were studied in the pseudorapidity range $|\eta^{jets}| < 2.4$. Furthermore, these events were studied in two different n-jet invariant mass regions, namely, $25 < M_{n-jets} < 50$ GeV and $M_{n-jets} > 50$ GeV, referred to as the low- and high-mass regions, respectively. The cross sections of the three- and four-jet low- and high-mass samples were measured differentially.

The data were compared to predictions from two $\mathcal{O}(\alpha\alpha_s)$ matrix element MC programs supplemented with parton showers, HERWIG 6.505 [8–10] and PYTHIA 6.206 [11], both with and without MPI. In the case of HERWIG , MPI events were simulated via an interface to JIMMY 4.0 [12], which is an impact parameter dependent model. For PYTHIA , MPI were generated using the so-called "simple model" [13].

In addition, the three-jet sample was compared to the fixed order ($\mathcal{O}(\alpha\alpha_s^2)$) calculation by Klasen, Kleinwort und Kramer [14]. This calculation corresponds to the three-jet LO and, at the time, was the highest order prediction available in photoproduction. Thus, no calculation was available for the four-jet sample.

The three- and four-jet cross sections are shown as a function of M_{n-jets} in figure 1. In general, both cross sections decrease exponentially with increasing M_{n-jets}. The HERWIG and PYTHIA predictions with and without MPI are also shown. They are normalized to the high invariant n-jets mass region ($M_{n-jets} > 50$ GeV), i.e. they are scaled to describe the high M_{n-jets} cross section. Both HERWIG and PYTHIA without MPI fail to describe the cross section dependence. When MPI are included, however, they are in quite good agreement with data. The discrepancy is larger in the four-jet case. The PYTHIA model was run using its default setting whereas the JIMMY model was tuned to the presented data [6].

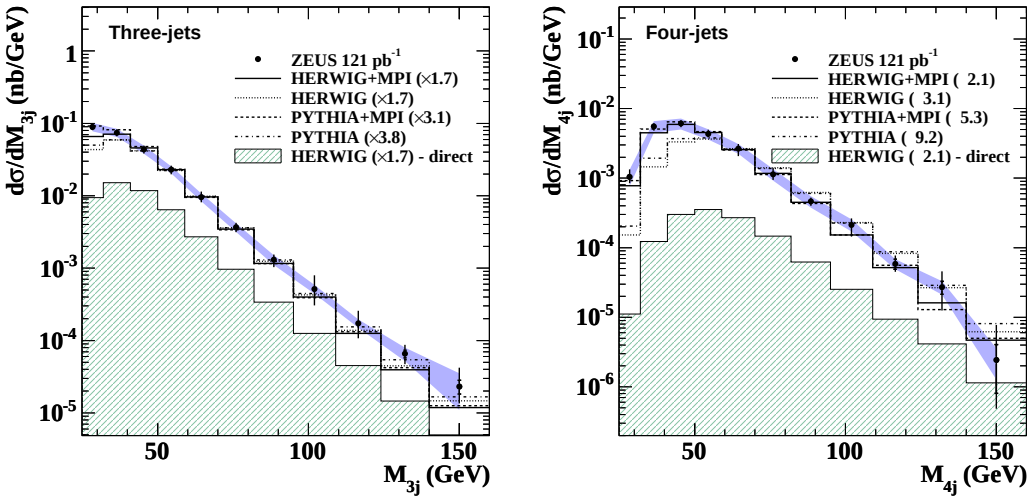

Fig. 1: Measured cross section as a function of (a) M_{3-jets} and (b) M_{4-jets} (solid circles). The inner and outer error bars and the shaded band represent the statistical, the statistical and the systematic added in quadrature and the calorimeter energy scale uncertainties, respectively.

Shown in Fig. 2a) is the measured three-jet cross section as a function of M_{3-jets}, compared to the fixed LO calculation for this process, $\mathcal{O}(\alpha\alpha_s^2)$. This calculation was corrected for hadronisation effects and MPI. The hadronisation and MPI corrections and their estimated uncertainties are shown in 2b). The hadronisation corrections are constant in M_{3-jets}, while MPI corrections increase towards low M_{3-jets}. The theoretical uncertainties on both the MPI corrections and the pQCD predictions are large. The magnitude and the shape of the calculation is consistent with the data within the large theoretical uncertainties. This is best seen in Fig. 2c) where the ratio data over theory is shown. Without the large MPI corrections the theoretical description would be far much worse at low M_{3-jets}.

3 Charged particle multiplicity in photoproduction

As described above, in quasi-real photoproduction ($Q^2 \sim 0$) the photon can develop a hadronic structure, where remnant-remnant interactions may be present and therefore the particle production can be enhanced. However, the actual particle multiplicity depends not only on the number of multiple parton scatterings but also on the hadronisation and on the colour connections between

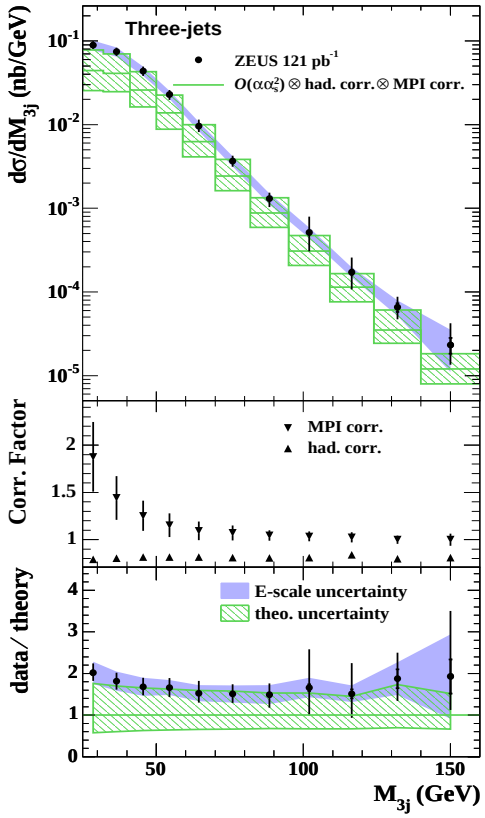

Fig. 2: (a) Measured three-jets cross section as a function of M_{3-jets} compared with an $\mathcal{O}(\alpha\alpha_s^2)$ prediction, corrected for hadronisation and MPI effects. (b) The hadronisation and MPI correction factors as a function of M_{3-jets}. (c) The ratio of the M_{3-jets} cross section divided by the theoretical prediction. The theoretical uncertainty is represented by shaded bands.

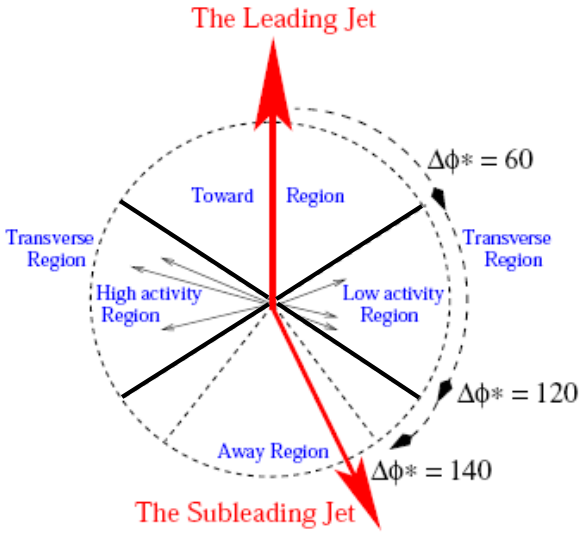

Fig. 3: Definition of the four azimuthal regions. The toward region is defined by the leading jet and by this means defines the away and transverse regions. The scalar sum of the transverse momenta $P_t^{sum} = \sum_i^{tracks/HFS} P_T^i$ calculated in each transverse region defines the high and low activity region eventwise in the charged particle multiplicity and mini-jet analyses, respectively.

the multiple parton scatterings and the remnants. Within the model used [15], different colour connection scenarios are possible. Two scenarios are studied. In the first scenario, each hard scattering is independent of the other and therefore is connected only to the remnants, which gives long colour strings. In the second scenario, the colour strings are rearranged in order to provide shorter strings, i.e. the hard scatterings are colour connected with each other, which compared with the first scenario produces fewer particles.

This was studied in the H1 collaboration by using a dijet photoproduction sample, where $Q^2 < 0.01$ GeV^2 and $0.3 < y < 0.65$, looking at charged particles with transverse energies $P_T^{track} > 150$ MeV in the pseudorapidity range $|\eta^{track}| < 1.5$. The jets were defined using the k_T clustering algorithm [7] and were required to have transverse momentum $P_T^{jets} > 5$ GeV and $|\eta^{jets}| < 1.5$.

Four regions in the azimuthal angle, ϕ, were then defined with respect to the leading jet as indicated in Fig. 3 in analogy to the CDF collaboration [16]. The leading jet (Jet_1) defines the toward region, whereas the subleading jet, the jet with the next highest P_T^{jet}, is usually in the away region, although not necessarily. The transverse regions are less effected by the hard interaction and thus, expected to be more sensitive to the MPI. For each event, the hemisphere which has the highest scalar sum of the transverse momenta, $P_t^{sum} = \sum_i^{tracks} P_T^i$, is refered to as the high-transverse-activity hemisphere. The other is referred to as the low-transverse-activity hemisphere.

The average track multiplicity, $\langle N_{charged} \rangle$, is shown in figures 4 and 5 as a function of $P_T^{Jet_1}$ for resolved photon enriched events, $x_\gamma^{obs} < 0.7$ (left) and direct photon enriched events, $x_\gamma^{obs} > 0.7$ (right). In the toward and away regions, the average track multiplicity increases with

$P_T^{Jet_1}$ as shown in figure 4. In the $x_\gamma^{obs} > 0.7$ region (right) the measurements are reasonably well described by the simulation containing only one hard interaction with parton showers and hadronisation, whereas in the region $x_\gamma^{obs} < 0.7$ (left) this is clearly not enough, especially at the lower values of $P_T^{Jet_1}$. MPI contributes as a pedestal and brings the prediction to a good agreement with the measurement.

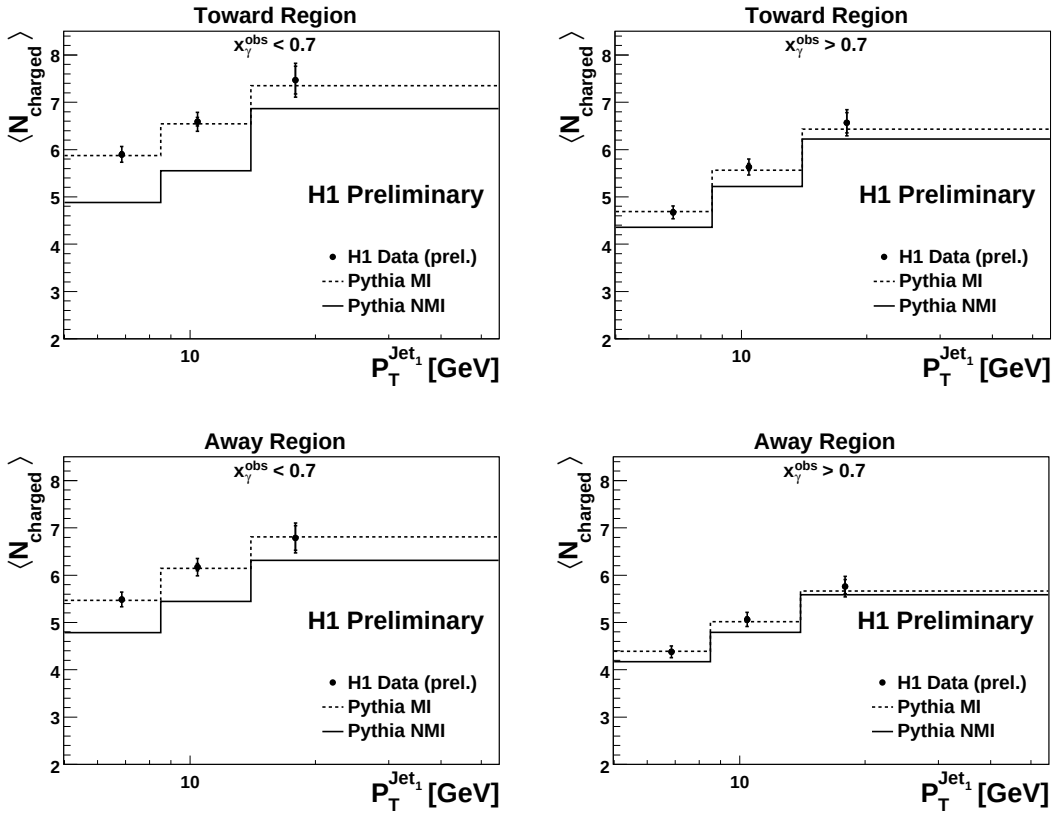

Fig. 4: Charged particle multiplicity for $x_\gamma^{obs} < 0.7$ (left) and for $x_\gamma^{obs} > 0.7$ (right). The leading jet (Jet_1) is contained in the toward region, whereas the subleading jet, the second jet with highest P_T^{jet}, is usually in the away region, although not necessarily. Data is compared to PYTHIA with and without MPI.

In the transverse regions, shown in figure 5, the measured average track multiplicity decreases with $P_T^{Jet_1}$. At high x_γ^{obs} (right) the predicted average charged particle multiplicity with and without MPI also decreases with $P_T^{Jet_1}$, although only PYTHIA with MPI describes data. At low x_γ^{obs} (left) the PYTHIA prediction without MPI tends to increase with $P_T^{Jet_1}$ while PYTHIA with MPI decreases with $P_T^{Jet_1}$ giving the best description of the data.

We studied[2] also the different colour string scenarios in Fig. 6 where the transverse regions are shown. In the present simulation the long string configuration is preferred.

[2]This is done in PYTHIA by the parameters PARP(86) = 0.66 and PARP(85) = 0.33, giving the probability that an additional interaction gives two gluons and the probability that an additional interaction gives two gluons with colour

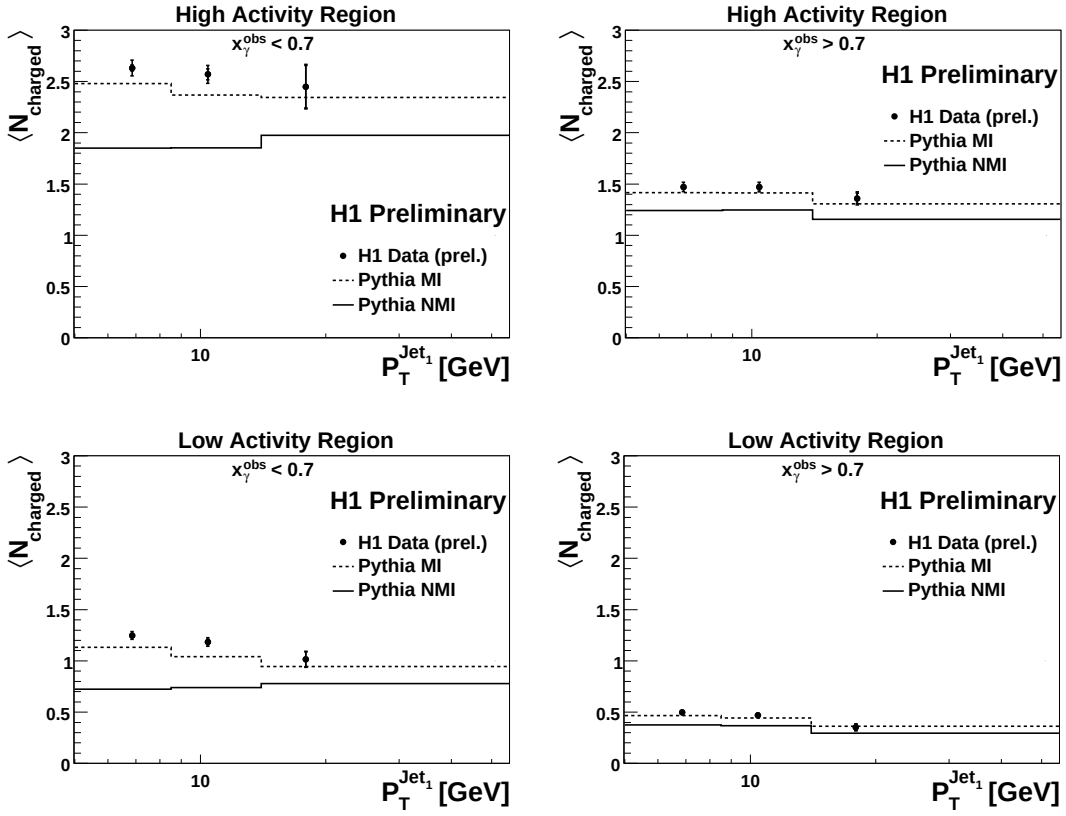

Fig. 5: Charged particle multiplicity for $x_\gamma^{obs} < 0.7$ (left) and for $x_\gamma^{obs} > 0.7$ (right). The transverse high activity regions, upper plots, are defined as the transverse region with a higher P_t^{sum} compared to the low activity regions, down. Data is compared to PYTHIA with and without MPI.

4 Mini-jet multiplicity in DIS

The photon is more likely to develop a hadronic structure before interacting with the proton in photoproduction than in DIS. In DIS, the characteristic interaction time scales like $\sim 1/Q^2$ and at high Q^2, it is too short for the fluctuations to occur. At HERA diffraction plays an important role at low x_{Bj}, and also at high Q^2. These events can be explained by the exchange of Pomerons. The AGK cutting rules relates the different contributions from diffraction and single or multiple parton scattering. Thus, it is interesting to study if evidence for multiple parton scattering can be seen within the data.

The H1 collaboration studied events in the kinematic region $5 < Q^2 < 100$ GeV^2 and $0.1 < y < 0.7$. Events with at least one jet with $E_T^{jet} > 5$ GeV and in the laboratory pseudorapidity range $-1.7 < \eta^{jet} < 2.79$ were selected[3] using the k_T clustering algorithm [7]. The HFS was required to have an invariant mass $W > 200$ GeV.

connections to nearest neighbours, respectively.

[3] Applied both in the hadronic centre-of-mass frame (HCM) and in the laboratory frames.

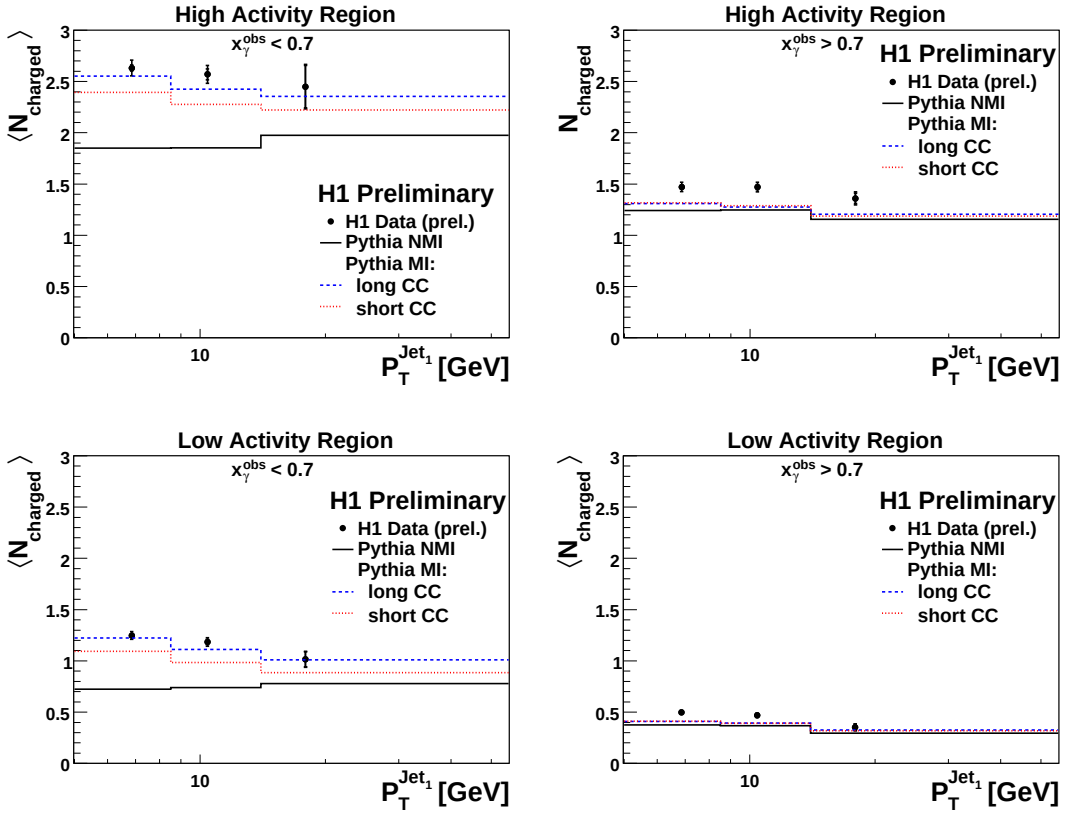

Fig. 6: Charged particle multiplicity for $x_\gamma^{obs} < 0.7$ (left), and for $x_\gamma^{obs} > 0.7$ (right). The transverse high activity regions, upper plots, are defined as the transverse region with a higher P_t^{sum} compared to the low activity regions, down. Here data is compared to PYTHIA without MPI and PYTHIA with MPI and high probability for long colour string connections, long CC, and short colour string connections, short CC.

The leading jet defines a toward, an away and two transverse regions (Fig. 3). The average multiplicity of jets with $E_T^{mini} > 3$ GeV, the so-called mini-jets, was measured, $\langle N_{minijet} \rangle$ in the range $-1.7 < \eta < 2.79$ for the four $\Delta\phi^*$ regions. A possible signature of MPI would be an increased value of $\langle N_{minijet} \rangle$, especially in the less populated high- and low-activity transverse regions and for the lower Q^2 values.

In Figure 7 the measured average mini-jet multiplicity is shown as a function of the transverse momentum of the leading jet in the hadronic centre-of-mass (HCM) frame, $P^*_{T,1j}$. The data are compared to the predictions of RAPGAP [17], ARIADNE [18] and PYTHIA . The former two do not include MPI whereas PYTHIA was run both with and without MPI.

The toward region data are reasonably well described by all four MC. While RAPGAP and PYTHIA
marginally underestimate $\langle N_{minijet} \rangle$ at low $P^*_{T,1j}$ in the lowest Q^2 bin ARIADNE slightly overestimates the data. The PYTHIA description is improved by the introduction of MPI at low Q^2.

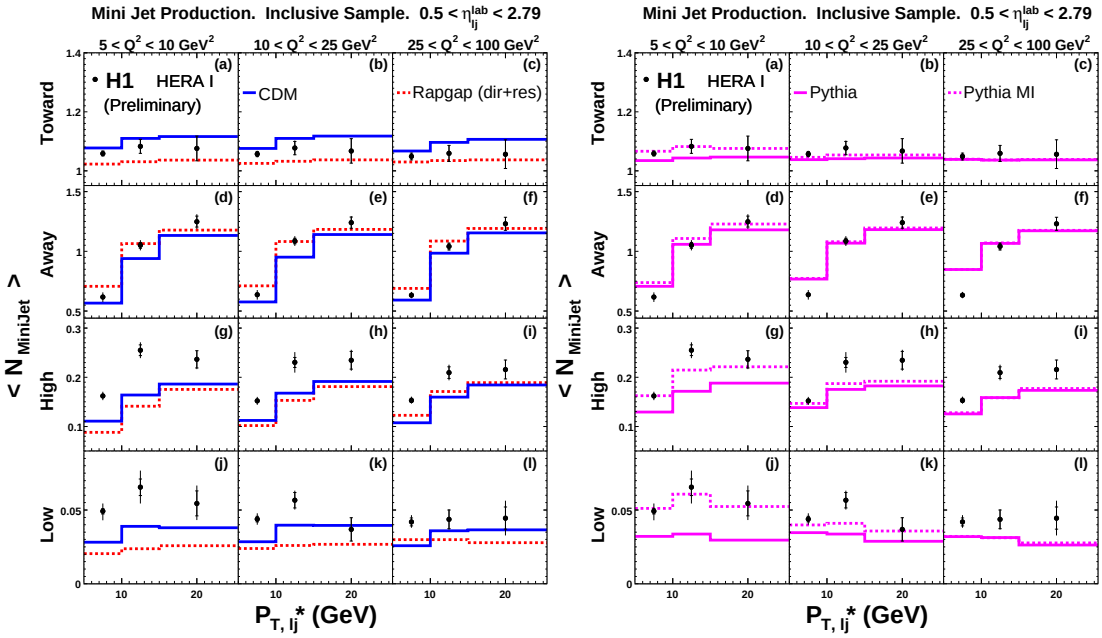

Fig. 7: The $\langle N_{minijet} \rangle$data, in all four azimuthal regions, as a function of $P^*_{T,1j}$ in three Q^2 bins. Also shown are the predictions from four MC models.

The overall description in the away region is good. The PYTHIA model predicts the away region to be the least sensitive to MPI. In the low and high activity transverse regions all the MC that do not include MPI underestimate the data in all $P^*_{T,1j}$ and Q^2 bins. This is more pronounced at low $P^*_{T,1j}$ and Q^2 values. The introduction of MPI in PYTHIA certainly aids in the description of the low Q^2 data. However, at large Q^2 the effect of MPI is very small according to the simulation and so PYTHIA underestimates the Q^2 data.

5 Conclusions

In all three analyses, both in photoproduction and in DIS, contributions from MPI are suggested. The three- and four-jet photoproduction cross sections shapes cannot be described by the $\mathcal{O}(\alpha\alpha_s)$ plus parton shower calculations. In the three-jet case the LO pQCD calculation needs to include the estimated hadronisation and MPI effects to describe data, where the latter has a large contribution towards low M_{3-jets}.

Both the charged particle and the mini-jet multiplicities are larger than predicted by MCs not including MPI. More specifically, the charged particle multiplicity as a function of $P_T^{Jet_1}$ predictions have a different shape depending on whether MPI is included or not in the transverse regions for low x_γ^{obs} values as seen by PYTHIA . The multiplicity can be only described in all regions properly when MPI are included. In the mini-jet analysis, the measured multiplicity is larger than the predictions by the parton shower and colour dipole model MCs. MPI, as predicted by PYTHIA , helps to describe the distributions at low Q^2 values but does not contribute at higher virtualities.

Higher partonic activity than predicted by standard MC is seen by all three analyses. These effects are also seen in DIS and at low and moderate Q^2 can be reasonably well described by including MPI.

References

[1] Abramovsky, V. A. and Gribov, V. N. and Kancheli, O. V., Yad. Fiz. **18**, 595 (1973).

[2] Bartels, J. and Salvadore, M. and Vacca, G. P., Eur. Phys. J. **C42**, 53 (2005).

[3] Bartels, J. Prepared for Gribov-75: Memorial Workshop on Quarks, Hadrons, and Strong Interactions, Budapest, Hungary, 22-24 May 2005.

[4] Derrick, M. and others, Phys. Lett. **B348**, 665 (1995).

[5] Aid, S. and others, Z. Phys. **C70**, 17 (1996).

[6] Namsoo, T., *Three- and Four-Jet States in Photoproduction at HERA.* Ph.D. Dissertation, Bristol University, September 2005.

[7] Catani, S. and Dokshitzer, Yuri L. and Seymour, M. H. and Webber, B. R., Nucl. Phys. **B406**, 187 (1993).

[8] Corcella, G. and others, JHEP **01**, 010 (2001).

[9] Corcella, G. and others (2002).

[10] Marchesini, G. and others, Comput. Phys. Commun. **67**, 465 (1992).

[11] Sjostrand, Torbjorn and Lonnblad, Leif and Mrenna, Stephen (2001).

[12] Butterworth, J. M. and Forshaw, Jeffrey R. and Seymour, M. H., Z. Phys. **C72**, 637 (1996).

[13] Sjostrand, Torbjorn and Mrenna, Stephen and Skands, Peter, JHEP **05**, 026 (2006).

[14] Klasen, Michael, Eur. Phys. J. **C7**, 225 (1999).

[15] Sjostrand, Torbjorn and van Zijl, Maria, Phys. Rev. **D36**, 2019 (1987).

[16] Acosta, Darin E. and others, Phys. Rev. **D65**, 072005 (2002).

[17] Jung, Hannes, Comp. Phys. Commun. **86**, 147 (1995).

[18] Lonnblad, Leif, Comput. Phys. Commun. **71**, 15 (1992).